

Bogdan WOŹNIAK, Ryszard HAPTER, Barbara MAJ

Polish Academy of Sciences  
Institute of Oceanology — Sopot

## THE INFLOW OF SOLAR ENERGY AND THE IRRADIANCE OF THE EUPHOTIC ZONE IN THE REGION OF EZCURRA INLET DURING THE ANTARCTIC SUMMER OF 1977/78 \*

### 1. INTRODUCTION

Solar energy affects the majority of fundamental and complex processes occurring in the sea either indirectly or directly. One of the most important interactions of light and the marine environment is its influence on the aquatic biosphere. Light, affecting the photosynthesis directly, determines primary production of the biomass in the sea, thus affects population of all living organisms. Responses of the organisms to photic impulses (phototropism), constituting one of the factors determining their migration and distribution in a basin, are also important.

In this connection it seemed worthwhile to include optical measurements of energetic characteristics of the light field in the sea in the programme of oceanographic and biological research carried out by the Second Polish Antarctic Expedition in Ezcurra Inlet during the Antarctic summer of 1977/78. As analysis of the results of measurements concerned both with the influx of the solar radiation to the sea surface and its diffusion into the water body is the subject of this paper.

Both spatial and spectral distributions of solar energy in a basin vary with the external solar flux reaching its surface (determined by geographical situation, season of the year, time of day, optical condi-

\* These studies were carried out under the research program MR II 16 coordinated by the Institute of Ecology of the Polish Academy of Sciences. They were sponsored in part under research program MR I 15 coordinated by the Institute of Hydro-Engineering of the Polish Academy of Sciences.

tions in the atmosphere etc.) and specific optical properties of the sea, characteristic for a particular region. As far as the Antarctic waters are concerned, this problem has been little studied. As yet, the investigations were limited for all practical purposes to atmospheric actinometric measurements (with the exception of a few papers [9, 16] also confined to studies of the optical properties of the sea in the Antarctic region) carried out systematically for several years at meteorological stations situated in that region [14]. These actinometric data refer only, however, to the whole range of solar energy falling on the sea surface. The main purpose of this work to give a full description of the inflow of solar energy to the basin studied (in particular to the euphotic zone), including both the magnitude of the radiant energy falling on its surface and that reaching particular depths.

To attain this goal, the actinometric measurements had to be supplemented with systematic monitoring of the optical properties of the sea, in particular the time-space fluctuations of spectral distributions of the irradiance attenuation coefficient with depth. Hence, the results of the investigations of energetic conditions occurring in the euphotic zone of Ezcurra Inlet also shed some light on the environmental optical properties of this basin.

All energetic and optical characteristics of underwater light fields presented in this paper were restricted to visible light over the wavelength range of 400—700 nm. Owing to strong attenuation of ultraviolet and infra-red in sea water, this range constitutes the major part of the solar energy penetrating the water body. Furthermore, for all practical purposes this range involves all the energy utilized in the photosynthesis of organic matter in the sea.

## 2. MATERIAL AND METHODS

The experiments were carried out in the region of Ezcurra Inlet from December 21st, 1977 to March 10th, 1978 (with the exception of 22—26 December, 6—14 and 28 January) on board the m.s. „Antoni Garnuszewski” anchored at a fixed position  $\varphi = 62^{\circ}10' S$ ,  $\lambda = 58^{\circ}32' W$ ) where the depth was 70—80 m. This paper presents the results of 65 all-day series of measurements of alternate above-water and underwater energetic characteristic of the solar radiation flux and meteorological observations. These included:

A) diurnal variations of irradiance (the definitions of all optical magnitudes used in the present paper have been discussed in detail in [2] and [7]),  $E_p$ . i.e. the magnitude of the solar energy over the whole

spectral range, reaching the sea surface through the atmosphere. The measurements were carried out by means of a universal M-80M pyranometer (made in the U.S.S.R.) calibrated in absolute power units ( $\text{W} \cdot \text{cm}^{-2}$ ). Time variations of  $E_p$  were registered by a recorder or digitally using electronic integrators and recording appliances equipped with a terminal printer (details of the methods, techniques and apparatus used for the optical and energetic characteristics of the light field by the team of optical physicists from the Polish Academy of Sciences' (PAS) Institute of Oceanology are described in [3, 10, 11, 17]). In the latter case, averaged irradiances over various time intervals could be determined owing to changes of integration times of electric signals from the pyranometer;

B) diurnal variations of underwater downward irradiance,  $E_d(\lambda, z)$  for the following seven wavelengths,  $\lambda$ , over the visible range: 425, 475, 500, 525, 550, 600 and 675 nm, were measured simultaneously at two different depths,  $z$ , in the sea. These measurements were carried out by means of two multichannel marine spectrophotometers (designed and made by the PAS' Institute of Oceanology), calibrated in absolute power units ( $\text{W} \cdot \text{cm}^{-2} \cdot \text{nm}^{-1}$ ). The depth of immersion of the optical sensors of the spectrophotometers was changed periodically and most frequently set at levels  $z_1 \approx 0 - 7$  m and  $z_2 \approx 15 - 25$  m. The choice of these depths was determined by the sensitivity thresholds of the sensors and irradiation of the basin, as well as by the desire to carry out the measurements within as thick a layer of euphotic zone as possible. The photo-currents from the optical sensors were measured in the same manner as in the case of the  $E_p$  measurements;

C) diurnal variations of the degree of total cloudiness. These observations were made every hour on the hour G.M.T. during the day. Data obtained by meteorologists on board the m.s. „Antoni Garnuszewski” was also utilized.

On the basis of the above data, other parameters characterizing the light influx reaching the sea surface and light field in the water body were determined and analysed, such as:

A) spectra of the downward irradiance attenuation coefficient in the sea,  $K_d(\lambda)$ . Generally, the  $K_d$  coefficients also depend on the depth and can be described by the equation

$$K_d(\lambda, z) = -\frac{1}{E_d(\lambda, z)} \frac{\partial E(\lambda, z)}{\partial z} \quad (1)$$

As the coefficients in this paper were determined by irradiance measured at two depths,  $z_1$  and  $z_2$ , they were computed from an appropriately transformed equation (2):

$$K_d(\lambda) = \frac{\ln[E(\lambda, z_1)/E(\lambda, z_2)]}{z_2 - z_1} \quad (2)$$

Hence, the  $K_d(\lambda)$  values can be considered to be the means for the layer bounded by the depths  $z_1$  and  $z_2$ . The  $K_d(\lambda)$  values, so determined, were assumed to be representative for the whole euphotic zone, the optical homogeneity of this zone being understood in terms of these  $K_d$  values;

B) spectra of downward irradiances,  $E_d(\lambda, z)$  at various (different from  $z_1$  and  $z_2$ ) depths in the euphotic zone of the sea. The magnitudes of these irradiances were determined from:

$$E_d(\lambda, z) = E_d(\lambda, z_1) e^{-K_d(\lambda, z)[z-z_1]} \quad (3)$$

on the basis of the measured irradiances,  $E_d(\lambda, z_1)$  and mean  $K_d(\lambda)$  coefficients calculated from eq. 2 for the euphotic zone;

C) irradiance,  $\overset{w}{E}_d(z)$ , over the visible range of the spectrum (400—700 nm) at various depths of the water body. These magnitudes were determined by numerical integration in respect of the wavelength of the  $E_d(\lambda, z)$  spectra, from the equation:

$$\begin{aligned} \lambda &= 700 \text{ nm} \\ E_d^W(z) &= \int_{\lambda=400 \text{ nm}}^{700 \text{ nm}} E_d(\lambda, z) d\lambda \end{aligned} \quad (4)$$

D) dose of solar energy over the whole spectral range, reaching the sea surface,  $\eta_p$ , and dose of the energy of visible light (400—700 nm) diffusing into particular depths of the water body,  $\eta_d(z)$ . These magnitudes were determined by integration over time  $t$  of temporal variations of the corresponding irradiances, according to the following relationships:

$$\eta_p = \int_{\Delta t} E_p(t) dt \quad (5)$$

$$\eta_d^W(z) = \int_{\Delta t} E_d^W(z, t) dt \quad (6)$$

Different time intervals,  $\Delta t$ , of the integration were assumed, depending on requirements (e.g. 1 hour, a whole day, etc.);

E) absolute transmission coefficients through the atmosphere,  $T$ , of diurnal doses of solar radiation. These magnitudes were determined from known  $\eta_p$  values:

$$T = \eta_p / \eta_{o,p} \quad (7)$$

where  $\eta_{o,p}$  is the dose of the solar energy falling on the upper layer of the atmosphere above the observation site in one day. The  $\eta_{o,p}$  values were determined from the equation: (8)

$$\eta_{o,p} = 480F[\arccos(-\operatorname{tg}\varphi \operatorname{tg}\delta) \sin\varphi \sin\delta + \frac{180}{\pi} \sin \arccos(-\operatorname{tg}\varphi \operatorname{tg}\delta) \cos\varphi \cos\delta],$$

where  $\eta_{o,p}$  is expressed in joules per unit area,  $F$  is the solar constant expressed in watts per unit area ( $F=1380 \text{ W} \cdot \text{m}^{-2}$ ),  $\varphi$  and  $\delta$ , expressed in degrees, are angles of latitude and solar declination, respectively. Equation (8) is obtained by integration over the time from sunrise to sunset of the expression for the time variability of solar irradiation on the top of the atmosphere:  $E(t)=F \cos\vartheta(t)$ , where  $\vartheta(t)$  is the time-dependent zenith distance of the sun;

F) average (for particular days and mean in the surface water layer from  $z=0$  to 30 m) attenuation coefficients of irradiance (400—700 nm)

with depth in the sea,  $K_d^w$ . These were calculated from daily energy doses of light, determined for the 0 and 30-m depths from the relationship

$$K_d^w = \frac{\ln [E_d^w(z=0 \text{ m}) / E_d^w(z=30 \text{ m})]}{\Delta z} \quad (9)$$

where  $\Delta z=30 \text{ m}$ ;

G) average ranges of the euphotic zone for particular days,  $z_e$ . In accordance with the optical criterion for the range of this zone adopted here [2], it is the depth to which 1% of the light energy with the wavelength  $\lambda_m$  (immediately under the sea surface) reaches. The wavelength corresponds to the maximum light penetration depth, i.e. to the minimum value of the attenuation coefficient in the spectrum,  $K_d(\lambda)$ . In the waters investigated the  $\lambda_m$  value was 525 nm. Hence, the ranges were determined from:

$$z_e = \frac{\ln 100}{K_d(\lambda = 525 \text{ nm})} \quad (10)$$

where  $K_d(\lambda=525 \text{ nm})$  is the mean daily magnitude of this coefficient;

H) diurnal depth variations,  $z_c$ , to which a given quantity of visible light penetrates,  $E_d^w=\text{const}$ . The fixed values of this irradiance assumed

were 10, 5, 1, 0.1, 0.01 and 0.001  $\text{mW} \cdot \text{cm}^{-2}$  and the corresponding depths were determined from the equation

$$E_n^w(z_c) = \text{const} = E_d^w(z=0) P(z_c) \quad (11)$$

where  $P(z_c)$  is a function of light transmission over the 400—700-nm range through a layer limited by depths of 0 and  $z_c$  metres, described by the equation ([5], [16]):

$$P(z_c) = \frac{\int_{\lambda_1=400 \text{ nm}}^{\lambda_2=700 \text{ nm}} E_d(\lambda, z=0) e^{-K_d(\lambda) \cdot z_c} d\lambda}{\int_{\lambda_1=400 \text{ nm}}^{\lambda_2=700 \text{ nm}} E_d(\lambda, z=0) d\lambda} = \frac{E_d(\lambda, z=z_c)}{E_d(\lambda, z=0)} \quad (12)$$

Graphs of variations of the  $z_c$  levels corresponding to particular  $E_d^w = \text{const}$  values, as a function of time, are referred to as „isophotes”; H) mean degree of cloudiness (in a 0—1 grade scale) for particular days:

$$n = \bar{N}/8 \quad (13)$$

where  $\bar{N}$  is the mean cloudiness (in a 0—8 grade scale) taken from records made every hour on the hour from sunrise to sunset.

The above measured and calculated optical properties were used to analyze the inflow of solar energy to the sea surface and irradiation of the euphotic zone.

### 3. RESULTS

The measurements and calculations enabled the determination of both temporal fluctuations of magnitudes characterizing diurnal irradiance fields of the sea surface and euphotic zone, and respective light energy doses for particular days during the research period. Owing to the volume of material, however, it is impossible to present it in full here. Hence, only the most essential parameters have been given, these including diurnal doses of solar energy reaching the sea surface and representative depths of the euphotic zone, as well as mean optical magnitudes for the sea and atmosphere on particular days. These results (Table 1),

Table 1. Daily energy doses and mean daily parameters characterizing the inflow of solar energy to the sea surface and its propagation in the euphotic zone of Ezcurra Inlet during the summer of 1977/78

$\eta_p$ ,  $\eta_d^w$  are the daily doses of solar radiation reaching the sea surface and of the 400–700-nm visible light band reaching selected depths,  $z$ , in the water body, respectively;

$T$  – is the absolute transmission coefficient of the daily energy doses through the atmosphere;

$n_w$  – is the mean degree of cloudiness during the day (in the 0–1 scale);

$K_d$  – is the mean attenuation coefficient (in the 0–30-m layer) of the downward irradiance in the 400–700 nm visible light band;

$z_c$  – is the mean range of the euphotic zone during the day.

Tab. 1. Dzienne dozy energii i średnie dzienne wartości parametrów charakteryzujących dopływ promieniowania słonecznego do powierzchni morza i jego propagację w strefie eupotycznej fiordu Ezcurra latem 1977/78

$\eta_p$ ,  $\eta_d^w$  – odpowiednio dzienne dozy energii promieniowania słonecznego padającego na powierzchnię morza i światła widzialnego w paśmie 400–700 nm na wybrane głębokości  $z$  w toni wodnej;

$T$  – bezwzględny współczynnik transmisji dziennych dów energii przez atmosferę;

$n_w$  – średni (w dniu) stopień zachmurzenia (w skali 0–1);

$K_d$  – średni w warstwie 0–30 m współczynnik osłabiania oświetlenia odgórnego światłem widzialnym w paśmie 400–700 nm;

$z_c$  – średni (w dniu) zasięg strefy eupotycznej.

Date Data	$\eta_p$ [ $J \cdot cm^{-2}$ ]	$T$	$n$	$\eta_d^w [J \cdot cm^{-2}]$				$K_d^w$ [ $m^{-1}$ ]	$z_c$ [m]
				$z = 5m$	$z = 10m$	$z = 20m$	$z = 30m$		
1	2	3	4	5	6	7	8	9	10
21.12.77	2441	0.57	0.75	870	47.1	2.57	0.155	0.288	20
27.12.	1779	0.41	0.86	744	43.2	3.31	0.281	0.263	21
28.12.	2088	0.49	0.92	867	51.7	4.13	0.355	0.260	21
29.12.	2965	0.69	0.61	1195	85.4	8.24	0.883	0.240	23
30.12.	2588	0.61	0.79	1064	93.2	11.5	1.56	0.213	26
31.12.	2915	0.68	0.66	1197	95.8	10.6	1.28	0.228	24
01.01.78	2083	0.49	0.81	863	63.4	6.32	0.689	0.238	22
02.01.	2699	0.63	0.78	1134	68.9	5.39	0.450	0.261	21
03.01.	2650	0.63	0.75	1104	43.4	2.34	0.141	0.299	18
04.01.	1044	0.25	0.99	437	19.8	1.14	0.0710	0.291	19
05.01.	718	0.17	0.97	342	19.7	1.60	0.146	0.259	22
15.01.	1821	0.45	0.92	761	108	23.1	5.46	0.165	30
16.01.	3144	0.78	0.47	1303	114	14.7	2.11	0.214	27
17.01.	2326	0.58	0.59	967	70.7	8.16	1.11	0.226	23
18.01.	1384	0.35	0.92	574	73.9	14.6	3.15	0.174	28
19.01.	1427	0.36	0.89	588	53.6	8.13	1.52	0.199	27
20.01.	1760	0.45	0.68	729	58.3	7.14	0.987	0.220	26
21.01.	2189	0.56	0.64	901	68.3	8.53	1.23	0.220	24
22.01.	1062	0.28	0.93	429	31.8	3.48	0.431	0.231	25
23.01.	1154	0.30	0.99	460	37.7	4.30	0.562	0.225	25
24.01.	2565	0.67	0.73	1059	88.5	10.6	1.44	0.220	26
25.01.	1748	0.46	0.87	730	63.6	8.11	1.14	0.215	26
26.01.	1811	0.48	0.72	752	68.5	9.48	1.44	0.209	25
27.01.	1372	0.37	0.96	563	74.2	14.5	3.03	0.174	33
29.01.	2076	0.57	0.93	859	58.6	5.91	0.645	0.240	23
30.01.	351	0.10	1.00	147	7.21	0.524	0.0413	0.272	20

Table 1, cont.; Tab. 1, c.d.

1	2	3	4	5	6	7	8	9	10
31.01.	602	0.17	1.00	253	9.03	0.471	0.0273	0.304	18
01.02.78	1019	0.29	0.83	422	11.1	0.429	0.0184	0.335	16
02.02.	1763	0.49	0.92	739	24.6	1.19	0.0647	0.311	17
03.02.	1445	0.41	0.85	592	25.4	1.59	0.111	0.286	19
04.02.	875	0.25	0.91	366	20.0	1.61	0.144	0.261	21
05.02.	1237	0.36	0.74	506	41.1	5.85	1.10	0.204	34
06.02.	1176	0.35	0.93	487	44.4	5.94	0.877	0.211	27
07.02.	1272	0.38	0.87	534	28.6	2.20	0.190	0.265	21
08.02.	2150	0.65	0.86	480	27.8	2.35	0.233	0.256	22
09.02.	1073	0.33	0.84	440	27.9	2.58	0.267	0.247	23
10.02.	1360	0.42	0.87	564	38.6	3.94	0.446	0.238	24
11.02.	1040	0.32	0.86	432	28.0	2.67	0.284	0.244	23
12.02.	1759	0.55	0.88	735	45.6	4.07	0.407	0.250	22
13.02.	1591	0.51	0.83	657	38.8	3.26	0.305	0.256	22
14.02.	1041	0.34	0.89	432	24.4	1.93	0.170	0.261	21
15.02.	1708	0.56	0.69	695	48.4	4.90	0.549	0.238	23
16.02.	1696	0.56	0.82	706	89.2	17.2	4.01	0.172	30
17.02.	1817	0.61	0.72	740	44.1	3.85	0.376	0.253	21
18.02.	2419	0.82	0.57	981	73.5	8.30	1.05	0.228	23
19.02.	2350	0.80	0.67	956	90.6	13.2	2.17	0.203	26
20.02.	1762	0.61	0.78	722	93.4	18.5	4.11	0.172	31
21.02.	1047	0.37	0.83	435	87.0	31.0	12.6	0.118	44
22.02.	1501	0.53	0.87	621	66.4	10.7	1.92	0.193	28
23.02.	1040	0.38	0.96	435	48.9	5.83	0.932	0.205	25
24.02.	851	0.31	0.97	355	37.0	5.51	1.11	0.192	26
25.02.	1950	0.72	0.73	799	56.4	6.05	0.734	0.233	22
26.02.	1240	0.47	0.94	517	39.9	4.74	0.633	0.224	23
27.02.	1115	0.43	0.74	454	38.0	4.92	0.712	0.215	24
28.02.	1750	0.68	0.47	716	61.9	8.52	1.31	0.210	25
01.03.	522	0.21	0.92	217	17.4	2.18	0.304	0.219	23
02.03.	1637	0.66	0.72	673	46.9	5.22	0.643	0.232	22
03.03.	2394	0.96	0.25	964	61.0	5.80	0.622	0.245	21
04.03.	2023	0.84	0.52	822	97.2	18.0	3.85	0.179	28
05.03.	1038	0.44	0.81	448	34.7	4.11	0.555	0.223	23
06.03.	905	0.39	0.93	378	32.0	3.24	0.371	0.321	22
07.03.	1688	0.73	0.53	682	47.0	5.13	0.603	0.234	21
08.03.	1048	0.46	0.90	430	21.5	1.74	0.164	0.262	19
09.03.	212	0.95	0.71	865	43.3	4.54	0.583	0.243	20
10.03.	756	0.35	0.94	315	22.8	3.12	0.578	0.210	23

thus characterize the fluctuation of light fields over the whole research period. As far as the fluctuations of these magnitudes in a single day are concerned, illustrative situations typical for a particular period and location have been presented, supplemented with statistical data on diurnal variations of the parameters averaged for observations lasting several days and the whole research period. As in the analyses of the variations of these parameters for the whole period, neither cyclic regularities nor similarity of the values of parameters could be found in series of consecutive days, all statistical calculations referring to observations lasting several days were made for sets of days in particular month, irrespective of their number. These results are listed in Tables 2—5.

Table 2. Averaged (for observations lasting many days in particular months and the whole research period) daily energy doses and parameters characterizing the inflow of solar radiation to the sea surface and its propagation in the euphotic zone of Ezcurra Inlet.

The meaning of the symbols in particular columns is the same as in Table 1, the corresponding values denoting the means for selected observation periods. — The mean value is given in the upper fraction of each line and the standard deviation,  $\delta$ , in the lower one.

Tab. 2. Uśrednione (dla wielodniowych obserwacji w poszczególnych miesiącach i całego okresu badań) dzienne dozy energii i parametry charakteryzujące dopływ promieniowania słonecznego do powierzchni morza i jego propagację w strefie eupotycznej fiordu Ezcurra

Znaczenie symboli w poszczególnych kolumnach takie samo jak w tab. 1, przy czym odpowiednie wartości mają sens przeciętnych dla wyróżnionych okresów obserwacji. W każdej kolumnie oprócz średnich (góra liczba) podano odchylenia standardowe notowanych wartości parametrów (dolna liczba) —  $\delta$ .

Observation days Czas obserwacji	$\langle n_p \rangle$			$\langle n_d^w \rangle$				$\langle K_d^w \rangle$		$\langle \chi_c \rangle$ [m]
	[J · cm <sup>-2</sup> ]	$\langle \tau \rangle$	$\langle n \rangle$	[J · cm <sup>-2</sup> ]	$\zeta=0m$	$\zeta=10m$	$\zeta=20m$	$\zeta=30m$	[m <sup>-1</sup> ]	
1	2	3	4	5	6	7	8	9	10	
XII (21, 27–31)	2463	0.56	0.77	971	68.5	6.67	0.743	0.248	22	
	424	0.10	0.10	167	20.9	3.29	0.491	0.022	2	
I (1–5, 15–27, 27–31)	1708	0.43	0.84	706	56.9	7.61	1.257	0.231	24	
	761	0.18	0.15	305	29.0	9.67	1.312	0.039	4	
II (1–28)	1466	0.48	0.82	590	46.6	6.53	1.315	0.231	24	
	429	0.15	0.11	166	22.5	6.49	2.400	0.043	5	
III (1–10)	1222	0.60	0.72	579	43.4	5.31	0.827	0.228	22	
	655	0.25	0.22	243	21.6	4.42	1.019	0.021	2	
Total Łącznie	1632	0.49	0.81	665	51.6	6.69	1.160	0.232	23	
	675	0.18	0.15	258	26.5	5.72	1.801	0.037	4	

Czas obserwacji  
Ogółem 2400

2011-08-22

Czas obserwacji  
Ogółem 2400

2011-08-22

**Table 3.** Averaged (for observations lasting many days and the whole research period) daily variations of mean 1 — hour solar irradiance of the sea surface, in the whole spectral range,  $\langle E_p \rangle_{in}$ , in the region of Ezcurra Inlet together with standard deviations,  $\delta$ , of the observed irradiance values.

**Tab. 3.** Przeciętne (dla wielodniowych obserwacji w poszczególnych miesiącach miesiąca) przebiegi w ciągu dnia wartości średnich godzinnych oświetlenia promieniowaniem słonecznym w całym zakresie widmowym, powierzchni morza  $\langle E_p \rangle_{in}$  w rejonie fiordu Ezcurra wraz z odchyleniami standaryзовanymi,  $\delta$ , notowanymi wartością tych oświetleń.

Observation days Czas obserwacji	Irradiance $\langle E_p \rangle_{in}$ [mW · cm <sup>-2</sup> ]												Oświetlenie $\langle E_p \rangle_{in}$ [mW · cm <sup>-2</sup> ]											
	2.00	3.00	4.00	5.00	6.00	7.00	8.00	9.00	10.00	11.00	12.00	13.00	14.00	15.00	16.00	17.00	18.00	19.00	20.00	21.00	22.00	23.00		
XII 21, 27-31 $\delta$	0.06	3.45	5.46	21.47	30.18	32.95	38.77	55.79	53.65	60.50	75.30	68.29	58.0	50.78	41.99	32.97	13.08	10.51	8.57	3.41	1.48	0.10		
	2.26	7.01	15.82	20.18	20.82	24.34	23.09	23.30	21.78	15.09	11.67	11.38	8.35	13.34	9.48	4.79	2.92	2.81	2.4	1.22				
I 1-5, 15-27, 29-31 $\delta$	0.06	1.52	3.22	7.33	13.78	19.44	25.93	33.27	45.41	53.81	57.77	47.11	46.42	34.98	30.16	23.56	16.15	8.53	3.90	2.30	0.50	0.03		
	1.21	2.18	5.42	9.95	12.25	17.19	18.30	25.88	32.85	33.93	23.17	25.27	17.50	16.42	12.39	9.38	5.49	2.52	2.31	0.38				
II 1-28 $\delta$	0.10	2.81	7.52	15.22	25.63	34.92	41.52	43.34	44.88	46.03	44.07	37.47	30.92	21.06	8.63	3.19	1.13	0.08						
	1.28	2.96	6.30	9.62	11.71	15.17	21.42	21.22	21.93	18.88	15.93	16.69	11.42	4.57	1.83	0.75								
III 1-10 $\delta$	0.42	4.98	20.89	37.98	44.66	56.88	54.55	46.55	42.57	32.67	25.40	16.25	7.88	0.38										
	0.41	2.62	17.05	20.21	21.61	21.66	21.45	23.75	20.75	18.25	13.20	7.57	2.93	0.13										
Total Łącznie $\delta$	0.02	0.81	1.59	5.56	10.54	16.64	26.21	36.78	44.38	50.39	53.21	48.51	45.88	37.16	30.85	22.23	11.35	5.16	2.54	1.25	0.30	0.02		
				11.35	12.57	11.93	17.36	21.18	24.26	27.18	24.55	21.33	16.97	16.33	11.84	7.32	4.59							

Table 4. Averaged (for observations lasting many days in particular months and the whole research period) statistical spectra of the downward irradiance attenuation coefficients,  $\langle K_d(\lambda) \rangle$ , together with standard deviations of these coefficients in a surface layer about 30 m thick of water body in Ezeurra Inlet.

Tab. 4 Uśrednione (dla wielodniowych obserwacji w poszczególnych miesiącach i dla całego okresu badań) statystyczne widma współczynników osłabiania oświetlenia odgórnego ( $K_d(\lambda)$ ), wraz z odchyleniami standardowymi notowanych wartości tych współczynników w powierzchniowej warstwie do ok. 30 m toni wodnej fiordu Ezeurra.

Observation days	Czas obserwacji	$\langle K_d(\lambda) \rangle$					
		$\lambda = 675 \text{ nm}$	$\lambda = 600 \text{ nm}$	$\lambda = 550 \text{ nm}$	$\lambda = 525 \text{ nm}$	$\lambda = 500 \text{ nm}$	$\lambda = 475 \text{ nm}$
XII 21, 27-31	0.292	0.248	0.210	0.198	0.230	0.317	0.569
	0.038	0.040	0.020	0.021	0.023	0.041	0.126
I 1-5, 15-27, 29-31	0.277	0.230	0.213	0.195	0.215	0.335	0.635
	0.046	0.039	0.035	0.031	0.037	0.027	0.130
II 1-28	0.235	0.226	0.213	0.197	0.203	0.336	0.658
	0.043	0.043	0.042	0.037	0.050	0.029	0.067
III 1-10	0.335	0.246	0.218	0.210	0.186	0.324	0.630
	0.065	0.048	0.023	0.021	0.018	0.015	0.071
Total	0.290	0.232	0.211	0.199	0.207	0.332	0.634
Lącznie	0.050	0.043	0.035	0.032	0.041	0.029	0.110

Table 5. Average (for observations lasting many days in particular months and the whole research period) values of mean 1-hour downward irradiance of the 400–700-nm visible light band,  $\langle E_d \rangle^w$ , at various depths,  $z$ , of the euphotic zone in Ezcurra Inlet — upper values, together with standard deviations of these values — lower values.

Tab. 5. Przeciętne (dla wielodniowych obserwacji w poszczególnych miesiącach oraz w całym okresie badań) wartości średnich godzinnych oświetlenia odgórnych,  $\langle E_d \rangle^w$ , światłem widzialnym w paśmie 400–700 nm na różnych głębokościach,  $z$ , strefy eupotycznej fiordu Ezcurra — gorna rzęba, wraz z odchyleniami standardowymi notowanymi wartością tych oświetleni — liczba dolna.

Obrzędowanie Czas obserwacji [dny]	z [m]	Irradiance $\langle E_d \rangle^w$ [mW·cm <sup>-2</sup> ]												Oświetlenie $\langle E_d \rangle^w$ [mW·cm <sup>-2</sup> ]						
		1				2				3				4			1			
		3.00	4.00	5.00	6.00	7.00	8.00	9.00	10.00	11.00	12.00	13.00	14.00	15.00	16.00	17.00	18.00	19.00	20.00	21.00
1	1	0.45	2.29	8.98	12.62	13.81	15.85	22.86	21.98	24.83	31.04	23.24	20.90	17.26	13.56	5.38	4.32	3.53	1.41	0.24
	0	0.93	2.83	6.46	8.24	8.48	9.82	9.29	9.32	8.74	6.41	5.01	4.91	3.45	5.42	3.85	1.11	1.18	1.17	0.24
XII	10	0.112	0.176	0.702	0.970	1.05	1.18	1.71	1.63	1.82	2.24	1.98	1.69	1.47	1.21	0.973	0.384	0.320	0.245	0.0989
	21,	0.086	0.226	0.531	0.685	0.69	0.77	0.83	0.81	0.77	0.69	0.37	0.33	0.27	0.42	0.330	0.098	0.102	0.072	0.0188
21, 27–31	20	0.0124	0.0189	0.0765	0.104	0.111	0.121	0.180	0.169	0.188	0.227	0.227	0.167	0.145	0.120	0.0971	0.0383	0.0305	0.0241	0.00979
	0	0.0109	0.0256	0.0611	0.079	0.079	0.0633	0.104	0.101	0.100	0.110	0.057	0.056	0.049	0.056	0.0467	0.0158	0.0117	0.0091	0.00248
30	0.00153	0.00227	0.00926	0.0124	0.0131	0.0139	0.0212	0.0198	0.0218	0.0261	0.0220	0.0189	0.0163	0.0135	0.0109	0.00433	0.00342	0.00270	0.00111	0.00037
	30	0.00150	0.00329	0.00776	0.0101	0.0100	0.0101	0.0145	0.0138	0.0145	0.0175	0.0093	0.0095	0.0084	0.0085	0.0072	0.00258	0.00186	0.00130	0.00037
0	1.35	2.69	5.74	8.09	10.79	13.84	22.33	23.90	21.59	19.33	14.57	12.57	9.85	6.72	3.51	1.63				
	0	0.91	2.19	4.11	5.05	7.09	7.56	10.67	13.48	14.13	13.07	10.43	7.24	6.82	5.14	3.92	2.22	1.05		
I	10	0.0977	0.246	0.479	0.674	0.833	1.14	1.50	1.74	1.90	1.74	1.52	1.19	1.00	0.778	0.552	0.256	0.136		
	1–5,	0.0736	0.191	0.396	0.500	0.644	0.75	0.96	1.02	1.20	1.20	0.93	0.70	0.57	0.452	0.451	0.251	0.122		
15–27, 28–31	20	0.0123	0.0326	0.0649	0.0910	0.117	0.154	0.198	0.218	0.251	0.235	0.198	0.158	0.129	0.100	0.0762	0.0410	0.0191		
	0	0.0096	0.0301	0.0670	0.0660	0.100	0.130	0.172	0.163	0.235	0.236	0.178	0.130	0.090	0.077	0.0940	0.0492	0.0247		
30	0.00180	0.00508	0.0106	0.0147	0.0186	0.0250	0.0319	0.0342	0.0415	0.0397	0.0323	0.0258	0.0205	0.0161	0.0130	0.00706	0.00335			
	30	0.00182	0.00620	0.0145	0.0178	0.0196	0.0266	0.0360	0.0336	0.0554	0.0559	0.0420	0.0301	0.0188	0.0169	0.0224	0.01137	0.00577		
II	0	1.14	3.05	6.17	10.37	14.08	16.78	17.86	18.01	18.50	17.71	14.94	12.17	8.04	3.79	1.26				
	0	0.54	1.25	2.80	4.01	4.72	6.26	8.95	8.61	8.32	7.54	5.85	6.28	3.96	1.70	0.66				
II	10	0.0051	0.228	0.480	0.522	1.13	1.34	1.42	1.46	1.40	1.17	0.93	0.596	0.281	0.0875					
	10	0.0470	0.117	0.309	0.322	1.13	1.34	1.34	1.46	0.93	0.80	0.60	0.544	0.314	0.138	0.0392				

Table 5, cont.

Tab. 5, cd.

1	2	3	4	5	6	7	8	9	10	11	12	13	14	15	16	17	18	19	20	21
20	0.0122	0.0376	0.0663	0.117	0.163	0.187	0.196	0.208	0.201	0.164	0.131	0.0796	0.0374	0.0111						
	0.0153	0.0342	0.0630	0.122	0.170	0.175	0.179	0.221	0.231	0.218	0.167	0.154	0.0748	0.0373	0.0104					
30	0.00265	0.00643	0.0102	0.0234	0.0332	0.0363	0.0367	0.0420	0.0424	0.0398	0.0333	0.0272	0.0151	0.00735	0.00211					
	0.00608	0.0134	0.0184	0.0402	0.0504	0.0542	0.0528	0.0770	0.0804	0.0807	0.0654	0.0624	0.0295	0.01478	0.00442					
0	0.176	2.08	8.61	15.53	18.36	23.32	22.37	19.06	17.50	13.49	10.62	6.81	3.31							
	0.165	3.05	7.36	8.48	8.71	8.70	8.60	9.54	8.33	7.34	5.32	3.06	1.19							
10	0.0137	0.146	0.631	1.11	1.34	1.67	1.62	1.38	1.30	1.03	0.816	0.517	0.254							
	0.0111	0.206	0.472	0.56	0.71	0.68	0.79	0.84	0.85	0.76	0.544	0.295	0.111							
20	0.00159	0.0177	0.0783	0.125	0.173	0.202	0.204	0.173	0.168	0.135	0.106	0.0663	0.0328							
	0.00147	0.0232	0.0718	0.094	0.133	0.134	0.164	0.159	0.164	0.144	0.102	0.0541	0.0196							
30	0.00024	0.00257	0.0121	0.0202	0.0257	0.0305	0.0321	0.0272	0.0272	0.0219	0.0170	0.0104	0.00517							
	0.00023	0.00413	0.0151	0.0209	0.0299	0.0315	0.0333	0.0361	0.0371	0.0321	0.0227	0.0120	0.00426							
0	0.134	0.648	2.19	4.36	6.87	10.74	15.04	18.18	20.79	21.79	20.48	18.77	15.15	12.53	8.95	4.81	2.10	0.852	0.130	
	0.103	0.332	0.181	0.345	0.544	0.845	1.18	1.41	1.60	1.70	1.59	1.45	1.18	0.964	0.677	0.374	0.165	0.0666	0.00913	
10	0.0114	0.00572	0.0228	0.0486	0.0709	0.111	0.157	0.187	0.203	0.223	0.192	0.156	0.125	0.0858	0.0483	0.0211	0.00840	0.0009		
	0.00014	0.00079	0.00346	0.00771	0.0117	0.192	0.2674	0.0317	0.0336	0.0388	0.0375	0.0335	0.0276	0.0222	0.0143	0.00859	0.00354	0.00133	0.0001	
30	0.00014	0.00079	0.00346	0.01660	0.0131	0.0236	0.0437	0.0430	0.0449	0.0616	0.0634	0.0502	0.0482	0.0436	0.0222	0.01620	0.00734			

Total

P<sub>accnle</sub>

#### 4. DISCUSSION

The results have been presented separately for: irradiance conditions at sea surface, attenuation coefficients of irradiance attenuation in the water body, and energetic characteristics of light fields in the euphotic zone.

##### 4.1. INFLOW OF SOLAR ENERGY TO THE SEA SURFACE

Energetic characteristics of light fields in the euphotic zone of a basin depend mainly on the absolute energy values of solar energy reaching its surface. Considerable differentiation and fluctuations of quantities of this energy were found to be characteristic for the case analyzed. These referred both to diurnal irradiation and all-day energy doses reaching the sea surface on particular days.

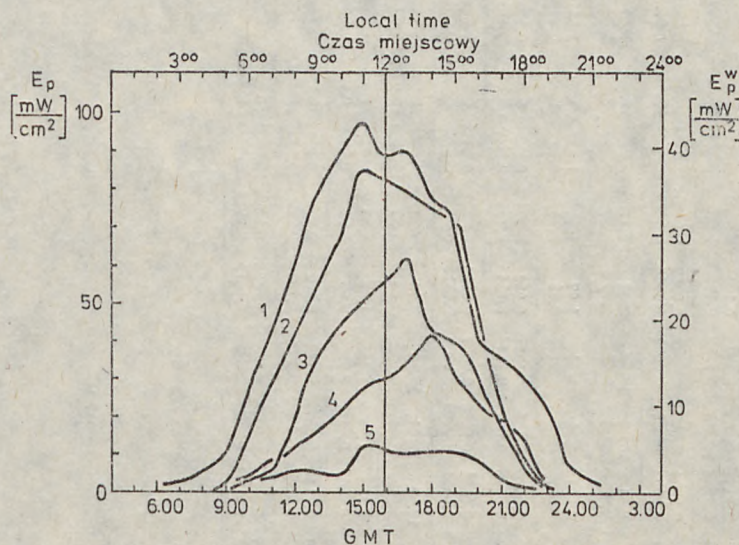


Fig. 1. Exemplary, typical and extremal diurnal variations (averaged for 1-hr time intervals) of the whole spectrum irradiance  $E_p$ , (left-hand scale) and the visible

(400–700 nm band) light irradiance  $E_p^w$ , (right-hand scale) of the sea surface. Curve numbers for particular days given: 1 — 16th January'78 (day on which the maximum daily dose of energy was recorded); 2 — 3rd March'78; 3 — 22nd February'78; 4 — 11th February'78; 5 — 31st January'78 (day on which the minimum daily dose of energy and maximum cloudiness were recorded).

Rys. 1. Przykładowe, typowe i skrajne dzienne przebiegi (średnione w jedno-godzinnych odcinkach czasowych) oświetlenia powierzchni morza promieniowaniem w całym zakresie widmowym —  $E_p$  (lewa skala) i światłem widzialnym w paśmie

400–700 nm —  $E_p^w$  (prawa skala)

Poszczególne krzywe dla dni: 1—16.I.1978 r. (dzień o maksymalnej dziennej dozie energii), 2—3.III.1978 r., 3—22.II.1978 r., 4—11.II.1978 r., 5—31.I.1978 r. dzień o minimalnej dozie energii i maksymalnym średnim stopniu zachmurzenia)

Fig. 1. illustrates the most typical and extreme diurnal variations (averaged for 1-hour intervals) of irradiance of the sea surface with the whole-spectrum radiation,  $\bar{E}_p$  (left-hand scale) and with the visible (400—700 nm) radiation,  $E_p^w$  (right-hand scale). The  $E_p$  values were estimated on the basis of the  $E_p$  values assuming ([1, 13, 15] and own data) the contribution of radiant energy over the visible range to total solar energy reaching the sea surface to amount to 44 per cent on average. As can be seen, the  $E_p$  values during the mid-day hours range over wide limits of 10—100 mW · cm<sup>-2</sup>, the differentiation thus being ten-fold. Still greater differences were noted for instantaneous irradiance values, not analysed in this paper. These were due to the extremely high instantaneous  $E_p$  values observed, which on days of medium cloudiness (2—4 of an 8-grade scale) and strong dynamic changes in the distribution of clouds showed substantial fluctuations, their short-term (from a couple to a dozen or so seconds) values exceeding that of the solar constant (138 mW · cm<sup>-2</sup>) considerably. These situations were caused by focussing of solar radiation on a selected point of the sea surface owing to reflection of the light from clouds and, to a lesser extent, from the slopes of glaciers surrounding Ezcurra fiord.

The graphs in Fig. 2 (according to Table 2) show averaged (over distinguished periods) diurnal variations of mean hourly irradiance of the basin surface,  $\langle E_p \rangle_{1h}$ , together with standard deviations, recorded in the Ezcurra Inlet region. The wide interval of standard deviations confirms the strong differentiation of irradiance during particular days which is characteristic for this region. Even so, their averaged variations appear to be typical for this region of the Antarctic, this being supported by comparison of the results for Ezcurra Inlet with those [14] for 1964—1965 obtained at a British actinometric station situated on the Argentina Islands ( $\varphi = 65^{\circ}15'$ ,  $\lambda = 64^{\circ}16'$  W), i.e. at a similar latitude. In these two regions, the irradiance is comparable, with the exception of this observed in March. In the latter case, however, the considerably higher mean irradiance values in Ezcurra Inlet, as compared with those determined in the Argentina Islands region, can be interpreted as being due to the period of measurements having been too short (10 days). Thus they can be considered as fortuitous and non-representative for the whole research period.

Rys. 2. Przeciętne (dla wielodniowych obserwacji w poszczególnych miesiącach i w całym okresie badań) zmiany w ciągu dnia średnich godzinnych oświetleń (sumarycznych) —  $\langle E_p \rangle_{1h}$  i światłem w paśmie widzialnym 400—700 nm —  $\langle E_p^w \rangle_{1h}$  powierzchni morza w rejonie fiordu Ezcurra (krzywe ciągłe), wraz z odchyleniami standardowymi notowanych wartości oświetleń (pionowe odcinki ciągłe).

Krzywe przerywane obrazują dla porównania podobne uśrednione przebiegi oświetleń wyznaczone na podstawie danych z pracy [14] dla rejonu Wysp Argentyńskich

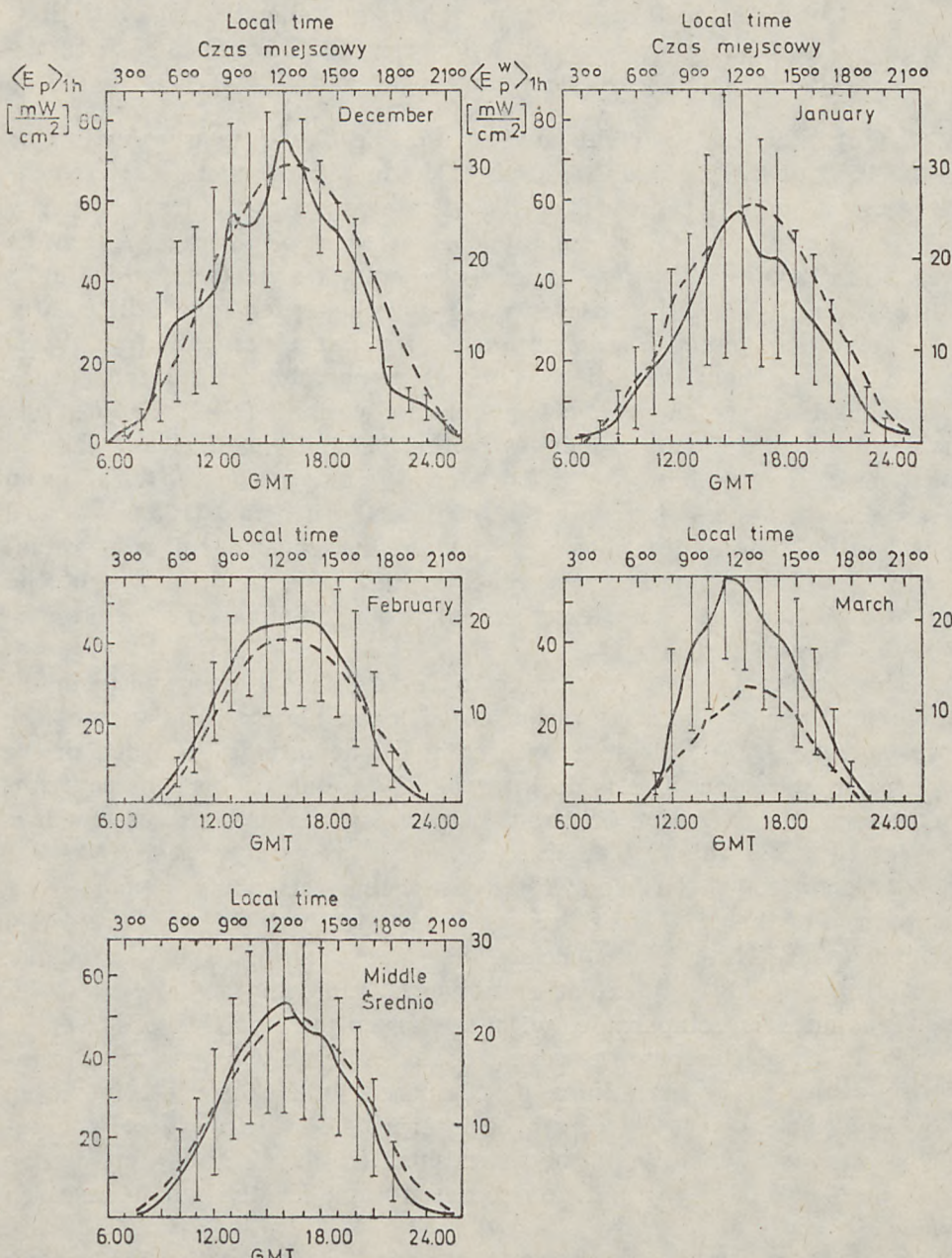


Fig. 2. Average (for observations lasting for periods of several days in particular months and the whole research period) diurnal variations of mean 1-hour irradiance (total) —  $\langle E_p \rangle_{1h}$  and with visible (400—700 nm band) light —  $\langle E_p^w \rangle_{1h}$  of the sea surface in the region of Ezcurra Inlet (continuous lines) together with standard deviations of the irradiance values (vertical bars). For comparison, the dashed curves show similar averaged irradiance variations for the region of the Argentina Islands [14].

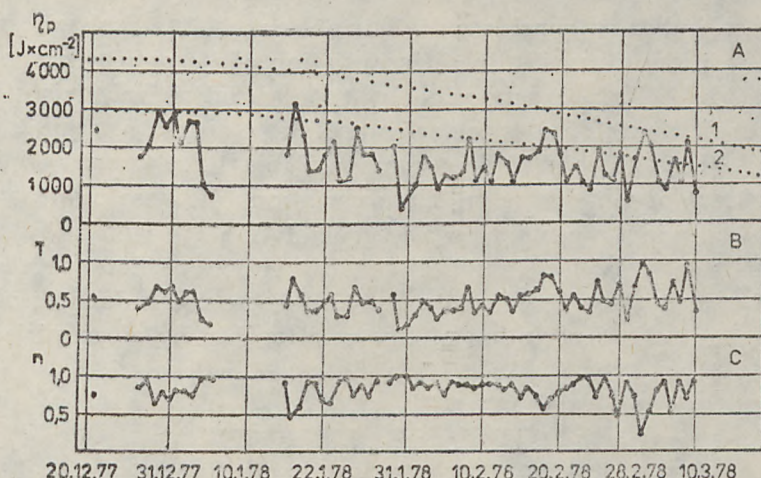


Fig. 3. Variations during the research period of: A — solar energy doses over the whole spectral range,  $\eta_p$ : a) those actually reaching the sea surface (continuous line), b) falling on the upper layers of the atmosphere above the observation site (dashed curve 1), c) with would have reached the sea surface in cloudless, standard atmosphere with the transmittance coefficient  $p_2=0.75$  (dashed curve 2); B — absolute transmission coefficients of diurnal radiant energy through the atmosphere ( $T$ ); C — mean diurnal degrees of cloudiness, ( $n$ )

Rys. 3. Zmiany w okresie badań: A — dół energii promieniowania słonecznego w całym zakresie widmowym  $\eta_p$ : a) docierających realnie do powierzchni morza (krzywa ciągła), b) padających na górne warstwy atmosfery nad miejscem obserwacji (krzywa przerywana 1), c) jakie docierałyby do powierzchni akwenu w warunkach bezchmurnej standardowej atmosfery ze współczynnikiem przeźroczystości  $p_2=0.75$  (krzywa przerywana 2); B — bezwzględnych współczynników transmisji całodziennych dów energii promieniowania przez atmosferę ( $T$ ); C — średnich dziennych stopni zachmurzenia ( $n$ )

The influx of solar radiation over the whole research period is illustrated (Fig. 3A, column 2 in Table 1) by actual diurnal doses of radiant energy,  $\eta_p$ , reaching the sea surface on particular days. For the sake of comparison, theoretical diurnal variations in solar energy doses reaching the upper layers of the atmosphere and variations of hypothetical doses of this energy that would have reached the sea surface in the cloudless standard atmosphere have also been included (during calculations for the standard atmosphere, a standard transparency coefficient of  $p_2=0.75$  was assumed, which corresponds to the optical mass of  $m=2$  [4, 6]. The method of calculations is described in detail, among others, in [1]).

The systematic decrease in theoretical doses (as well as average true doses in particular months — cf. column 2, Table 2) in the period from December and March was due to variations in sun declination. This is an obvious limitation of the absolute amount of energy reaching the sea surface by astronomical factors. On the other hand, the observed

time-independent dispersion of true values of energy doses reaching the sea surface indicates considerable fluctuations of atmospheric meteorological conditions resulting in differentiation of its optical properties on particular days. This is supported by time variations of absolute transmission coefficients of diurnal solar radiation doses through the atmosphere,  $T$ , (Figs. 3B and C according to Table 1, columns 3 and 4) and mean degrees of cloudiness,  $n$ . Time variations of these two magnitudes reveal, in addition, a certain negative correlation. As seen in Fig. 4, however, the relatively low number and dispersion of data points in the graph of transmission coefficients, as well as the mean degrees of cloudiness, preclude the description of this relationship by an empirical equation.

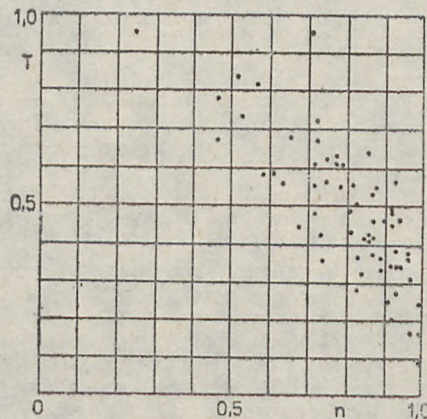


Fig. 4. Observed relationship between absolute transmission coefficient of diurnal solar irradiance doses ( $T$ ), and mean daily degrees of cloudiness ( $n$ )

Rys. 4. Obserwowana zależność bezwzględnych współczynników transmisji całodziennych dów energii promieniowania słonecznego —  $T$  od średnich dziennych stopni zachmurzenia —  $n$

Distributions of relative frequency of occurrence of rates cloudiness,  $n$ , of transmission,  $T$ , and diurnal energy doses reaching the sea surface,  $\eta_p$ , (on the probability density scale) during the whole research period, are shown in Fig. 5. Characteristic statistical parameters of these distributions (mean values and standard deviations) for both the whole research period and particular observations lasting for periods of several days, are listed in Table 2 (columns 2—4). It should be noted that the results do not show any regularities (of the cyclic type) in seasonal variations of meteorological conditions of the atmosphere, represented by the degree of cloudiness,  $n$ , and its optical properties described by the transmission coefficients,  $T$ . Respective mean values of these parameters for the successive periods distinguished (cf. Table 2) are quite fortuitous.

#### 4.2. IRRADIANCE ATTENUATION COEFFICIENTS IN THE EUPHOTIC ZONE OF THE SEA

Coefficients of diffuse attenuation of the downward irradiance provide fundamental optical parameters characterizing the diffusion of radiant energy into the basin. They describe fluctuations, both as regards spectral and absolute value terms, of the downward irradiance with

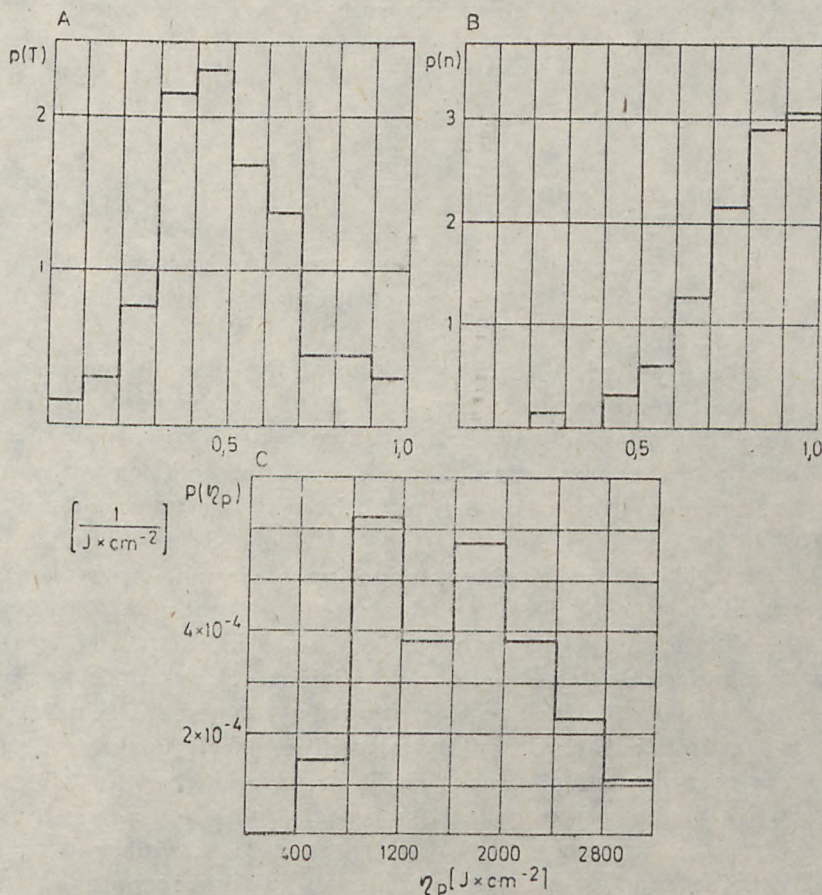


Fig. 5. Distribution of mean rates of occurrence of: A — absolute transmission coefficients of diurnal energy doses through the atmosphere ( $T$ ); B — mean daily degrees of cloudiness ( $n$ ); C — diurnal solar energy doses reaching the sea surface ( $\eta_p$ )

Rys. 5. Rozkłady względnych częstotliwości występowania wartości: A — bezwzględnych współczynników transmisji całodziennych dów energii promieniowania słonecznego przez atmosferę ( $T$ ); B — średnich dziennych stopni zachmurzenia — ( $n$ ); C — całodziennych dów energii promieniowania słonecznego padającego na powierzchnię morza ( $\eta_p$ )

depth, according to the following relations: monochromatic downward irradiance (falling within the narrow wavelength interval,  $\lambda - \lambda + \delta\lambda$ ):

$$E_d(\lambda, z) = E_d(\lambda, z=0) e^{-\int_0^z K_d(\lambda, z) dz} \quad (14)$$

downward irradiance over the visible range (i.e. a wide wavelength interval: 400—700 nm):

$$E_d^w(z) = E_d^w(z=0) e^{-\int_0^z K_d^w(z) dz} = E_d^w(z=0) e^{-K_d^w z} \quad (15)$$

where  $K_d(\lambda)$  and  $K_d$  are the mean downward irradiance attenuation coefficients in the  $0 - z$  layer, of monochromatic and visible light, respectively.

As has been stated, the mean values of the attenuation coefficient in the surface layer down to a depth of 30 m are discussed rather than continuous fluctuations of the coefficient with depth (analyses of spatial variations of monochromatic irradiance attenuation coefficient for several illustrative wavelengths have been published in this volume by Olszewski [12]).

The spectral nature of the attenuation of irradiance in the water body of the basin considered is illustrated by the mean spectrum of  $\langle K_d(\lambda) \rangle$  — for the total research period (Fig. 6 based on Table 4) together with standard deviations of the coefficients. For comparison, a similar spectrum characteristic for various optical types and classes of sea waters according to Jerlov's optical classification [7] has also been presented. As regards optical properties, the sea and oceanic waters were classified by Jerlov [7] into various types, from the cleanest oceanic waters (type I), through moderately transparent oceanic waters of the types IA, IB, II and III, to turbid and strongly turbid inshore waters (classes 1 through 9).

As can be seen, the minimum spectra of the attenuation coefficients in the spectra of the Ezcurra Inlet water body occurs within the 500—550 nm band (mean 525 nm; green light), which is characteristic for classes 1 through 5 of the inshore waters.

The absolute values of the coefficients also fall within the range characteristic for these classes. The shape of the  $K_d(\lambda)$  spectrum, however, differs markedly from those encountered in other seas. The difference consists in a considerably smaller slope of the curve in the short-wa-

wavelength range of the visible spectrum in Ezcurra Inlet than in other basins. This can be explained by the relatively small concentration of organic matter dissolved in sea water which strongly absorbs light within this portion of the spectrum. Thus, the high concentration of suspended matter (see the paper by Jonasz in this volume), which attenuates the light much more non-selectively in respect of the wavelength, mainly by scattering, plays a dominating role in light attenuation. This is also supported by Olszewski's results [12].

Observations have shown that waters of the basin considered exhibit strong time variations in the absolute values of optical parameters. Both distinct and rapid fluctuations of the momentary irradiance attenuation coefficients occurring from hour to hour, which were mostly irregular

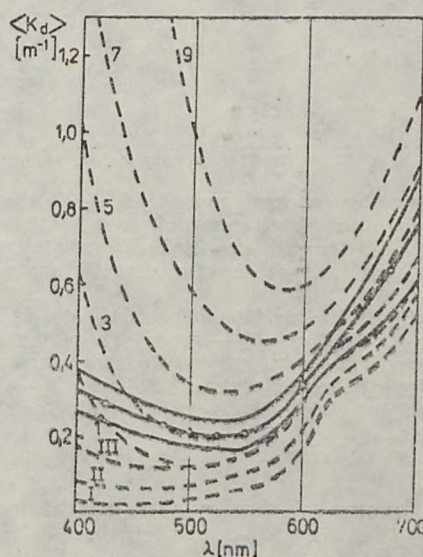


Fig. 6. Spectrum of downward irradiance attenuation coefficients in the surface layer of the basin: a) statistical means in the layer down to 30 m in Ezcurra Inlet — continuous curve; the shaded area shows the interval of standard deviations of the coefficient values; b) in various types of oceanic and sea waters according to Jerlov's classification [7] — dashed curve with numbers

Rys. 6. Wicmo współczynników osłabiania oświetlenia odgórnego w powierzchniowej warstwie akwenu: a) — średnie statystyczne w warstwie do 30 m we fiorze Ezcurra — krzywa ciągła; obszar zaciemiony ilustruje przedział odchyleń standardowych notowanych wielkości współczynników; b) w różnych typach wód oceanicznych i morskich wg klasyfikacji Jerlova [7] — krzywa przerywana z numerami.

and correlated only slightly with tidal cycles, and day-to-day variations of the mean diurnal values of these parameters were noted. The latter are shown in Fig. 7, where mean diurnal variations of attenuation coefficients of the downward irradiance over the visible range (400—700 nm)

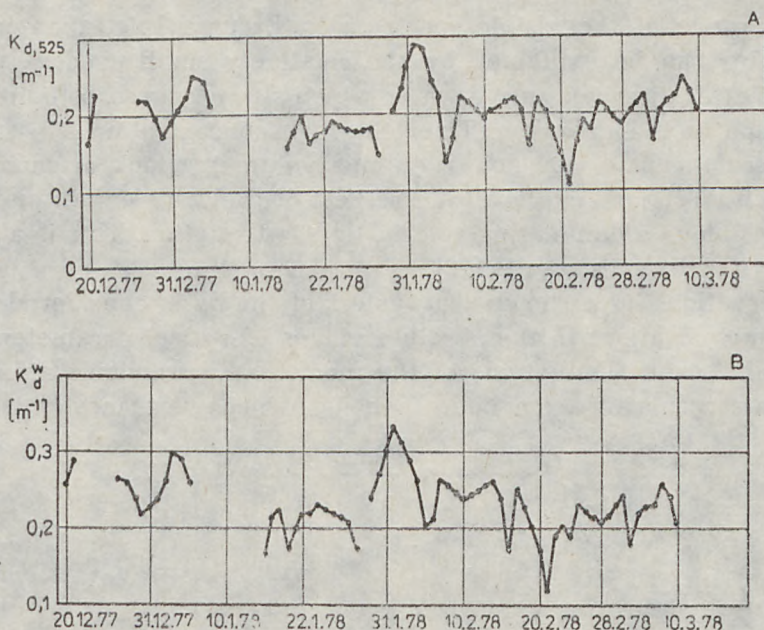


Fig. 7. Variations during the research period: A — of the mean (in the surface layer down to about 30 m) diurnal attenuation coefficient of the downward monochromatic irradiance  $K_{d,525}$ , for 525 nm light; B — of the mean (in the surface layer down to about 30 m) diurnal attenuation coefficient of the downward irra-

diance,  $K_d^w$ , for visible light within the 400—700 nm band

Rys. 7. Zmiany w okresie badań: A — średniego w warstwie powierzchniowej (do ok. 30 m) dziennego współczynnika osłabiania monochromatycznego oświetlenia odgórnego —  $K_{d,525}$ , dla światła o długości fali 525 nm; B — średniego w warstwie powierzchniowej (do ok. 30 m) dziennego współczynnika osłabiania oświetlenia odgórnego —  $K_d^w$  dla światła widzialnego w paśmie 400—700 nm

and exemplary monochromatic downward irradiance with the 525-nm light are presented. The scale of these variations is illustrated by distribution of relative rates of occurrence of particular coefficients shown in Fig. 8 which were determined for the whole research period. Characteristic statistical parameters of these coefficients (mean values and standard deviations) during the whole period and for particular time intervals are listed in Tables 2 (column 9) and 4.

It is worth noting that the analyses of the results did not reveal any regularity (of the cyclic type) in time variations of mean irradiance attenuation coefficients in the sea, on particular days, as was the case with optical properties of the atmosphere. A characteristic feature of these data (cf. Tables 2 and 4) is the substantial constancy of the mean, rather than diurnal values of the irradiance attenuation coefficients taken from observations lasting for periods of several days, thus the considerable day-to-day fluctuations of one-day mean values of optical parameters of

the sea water likely to be due to short-term (of the order of several days) local dynamic processes, such as intensified flow of glaciers, mixing of water masses, raising of the bottom material during storms, etc.). On the other hand, the constancy of the mean values for periods of several days over the whole observation period, indicates the possible global stability of the water masses in this basin owing to the restricted exchange of water with the ocean.

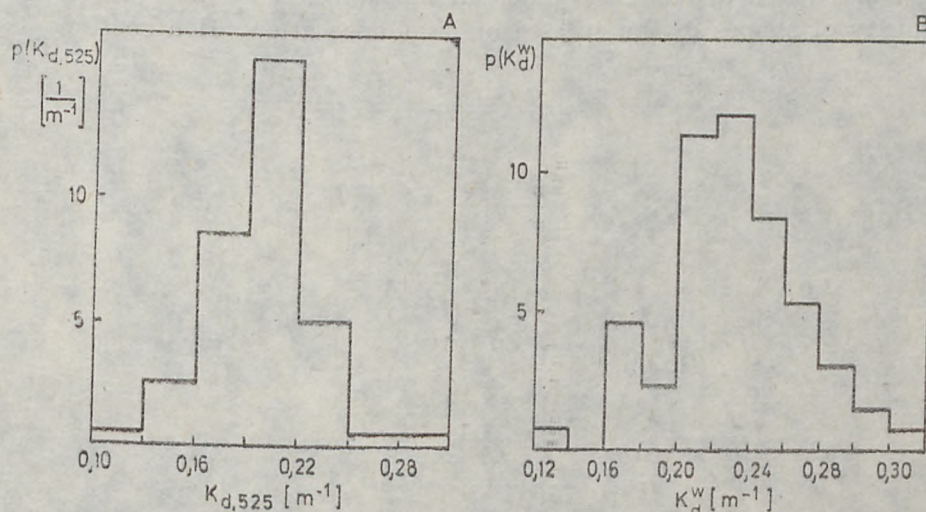


Fig. 8. Distribution of the mean rates of occurrence of: A — the mean (in the surface layer down to about 30 m) diurnal attenuation coefficient of the monochromatic downward irradiance,  $K_{d,525}$ , for 525 nm light; B — the mean (in the surface layer down to about 30 m) diurnal attenuation coefficient of the downward irradiance,  $K_d^w$ , for visible light within the 400–700 nm band

Rys. 8. Rozkłady względnych częstotliwości występowania wartości: A — średniego w warstwie powierzchniowej (do ok. 30 m) dziennego współczynnika osłabiania monochromatycznego oświetlenia odgórnego —  $K_{d,525}$  dla światła o długości fali 525 nm; B — średniego w warstwie powierzchniowej (do ok. 30 m) dziennego współczynnika osłabiania oświetlenia odgórnego —  $K_d^w$  dla światła widzialnego w paśmie 400–700 nm

#### 4.3. ENERGETIC CHARACTERISTICS OF THE IRRADIANCE FIELDS AND THE RANGE OF THE EUPHOTIC ZONE IN THE SEA

As mentioned in the introduction, energetic characteristics of the irradiance fields in the euphotic zone of a basin are determined by the total effect of attenuation of the solar radiation flux in the atmosphere and in the sea. As, in the case considered, the optical conditions in the two media fluctuated greatly during the period of research, a strong time-space differentiation of underwater irradiation fields was also observed. This referred both to the spectral composition of radiant energy pene-

trating into the basin and the absolute values of this energy which reaches particular depths in the sea.

Fig. 9 gives examples (extremes in Figs. A and C and intermediate in Fig. B) of spectral distributions of the downward irradiance,  $E_d(\lambda)$ , at various depths observed on various days noon. Apart from differences in absolute energy values, the common feature of irradiance distribution in all these cases is the predomination of the green light, this increasing with depth (with a maximum at about 525 nm). This follows from the similarity of shapes of the spectra of irradiance attenuation coefficients

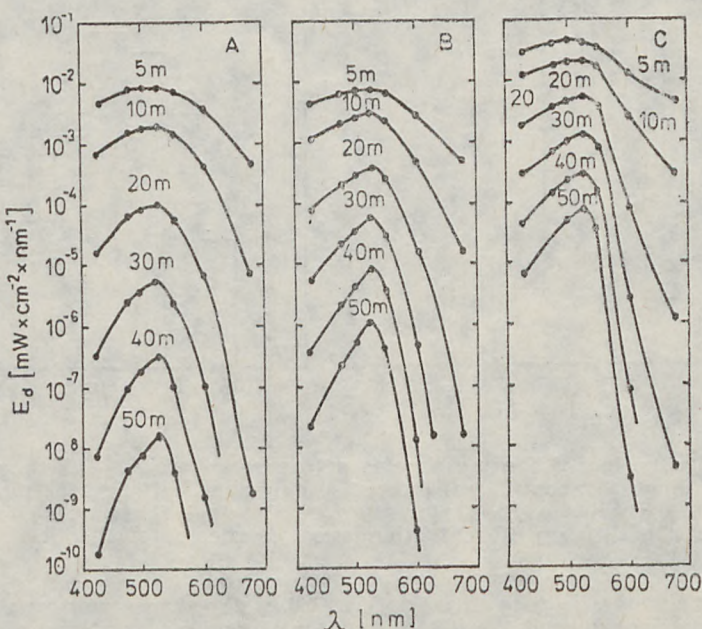


Fig. 9. Exemplary spectra of downward irradiance at selected depths in the basin, observed at midday on 1st Feb.'78 (A), 5th Feb.'78 (B) and 27th Jan.'78.

Rys. 9. Przykładowe widma oświetlenia odgórnego na wybranych głębokościach w akwenie obserwowane w południe: A — 1.II.1978; B — 5.II.1978; C — 27.I.1978

observed on different days during the period of research, which had a reasonably stable attenuation minimum for  $\lambda=525$  nm. On the other hand, the differentiation of the absolute values of the downward irra-

diance, both the monochromatic,  $E_d(\lambda)$  and visible,  $E_d^w$  (illustrated for the whole day in Fig. 10 where extremely different daily isophote values are shown) was due to fluctuations of irradiance conditions on the sea surface and variations in absolute irradiance attenuation coefficients in the water body.

The graphs in Fig. 11 show averaged diurnal variations of mean

1-hour downward irradiances over the 400—700-nm range,  $\langle E_d^w \rangle_{1h}$ , (for observations lasting several days in particular months and for the whole

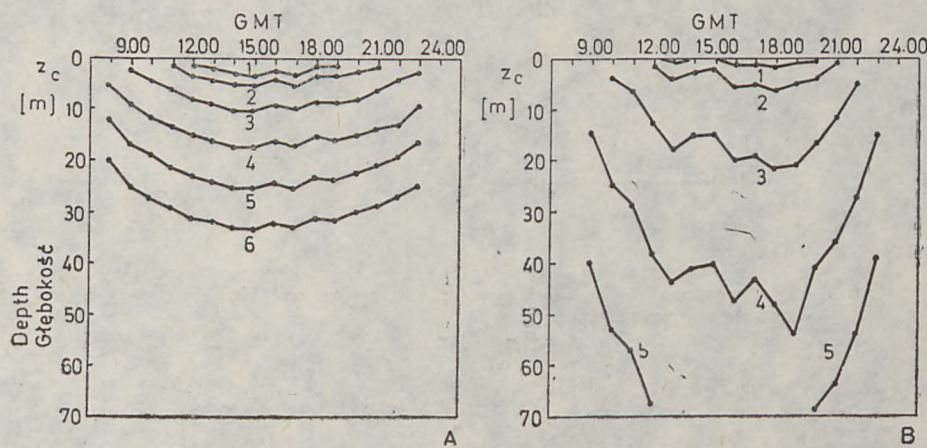


Fig. 10. Diurnal variations of the isophotes: 1 —  $10 \text{ mW} \cdot \text{cm}^{-2}$ ; 2 —  $5 \text{ mW} \cdot \text{cm}^{-2}$ ; 3 —  $1 \text{ mW} \cdot \text{cm}^{-2}$ ; 4 —  $0.1 \text{ mW} \cdot \text{cm}^{-2}$ ; 5 —  $0.01 \text{ mW} \cdot \text{cm}^{-2}$ ; 6 —  $0.001 \text{ mW} \cdot \text{cm}^{-2}$  observed on days with extremely different (low on 2nd Feb.'78 and high on 21st Feb.'78) irradiance levels in the water body

Rys. 10. Dzienne przebiegi izofot: 1 —  $10 \text{ mW} \cdot \text{cm}^{-2}$ , 2 —  $5 \text{ mW} \cdot \text{cm}^{-2}$ , 3 —  $1 \text{ mW} \cdot \text{cm}^{-2}$ , 4 —  $0.1 \text{ mW} \cdot \text{cm}^{-2}$ , 5 —  $0.01 \text{ mW} \cdot \text{cm}^{-2}$ , 6 —  $0.001 \text{ mW} \cdot \text{cm}^{-2}$  obserwowane w dniach o skrajnie różnych (niskich — 2.II.1978 i wysokich — 21.II.1978) poziomach oświetlenia w toni wodnej

observation period). Standard deviations of these values are listed in Table 5. As compared with the mean irradiance values, the very high standard deviation values confirm the observed great differentiation of energetic conditions in the water body on particular days, this differentiation increasing with depth. For instance, the standard deviations of irradiance recorded during the whole period at pre-determined hours at a depth of 0 m (immediately below the surface) were mostly about two times less than the mean values, whereas at a depth of 30 m they were about 1.2—2 times greater than the mean values.

The inflow of solar energy to the euphotic zone of the basin during the whole observation period is illustrated by all-day energy doses of the 400—700-nm light which reached different depths of the water body on particular days (Fig. 12 based on Table 1). There are strong, day-to-day, irregular variations of irradiance conditions in the basin, the dispersion of the light energy doses also increasing greatly with depth. For instance, in extremal cases the ratio of the maximum to minimum diurnal energy doses amounted to about 9 and more than 800 at depths of 0 and 30 m, respectively. The values of these doses, averaged for observations

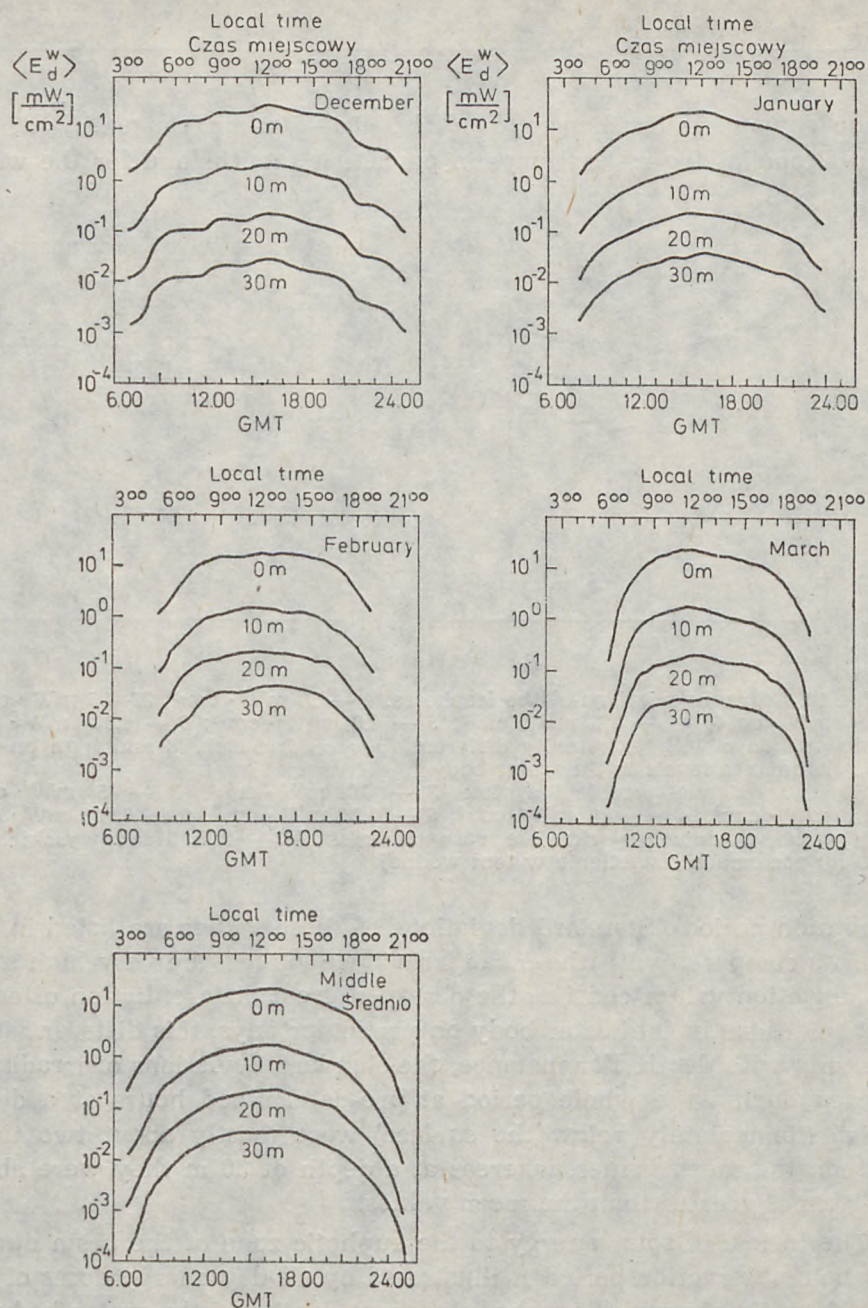


Fig. 11. Average (for observations lasting for a period of several days) in particular months and during the whole research period) variations during the day of the mean hourly downward irradiance in the 400—700 nm band — visible light,

$E_d^w$ , recorded at selected depths in the euphotic zone of the sea

Rys. 11. Przeciętne (dla wielodniowych obserwacji w poszczególnych miesiącach i w całym okresie badań) zmiany w ciągu dnia średnich godzinnych oświetleń od-

górnego światłem widzialnym w paśmie 400—700 nm —  $E_d^w$ , notowanych na wybranych głębokościach w strefie eufotycznej morza

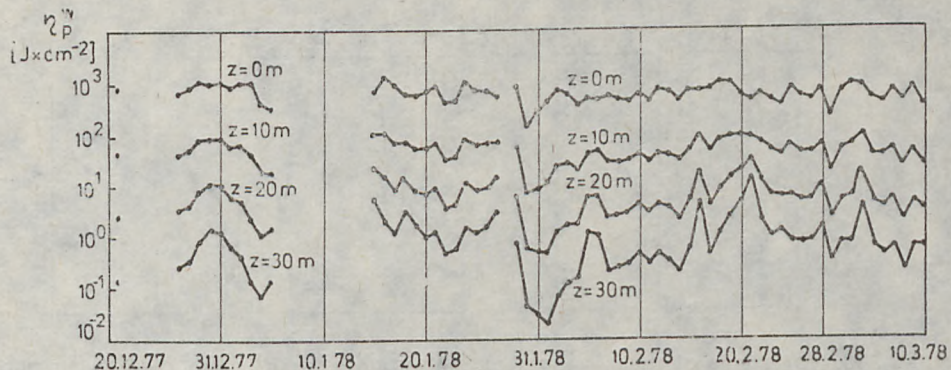


Fig. 12. Variations of diurnal visible (400—700 nm band) light energy doses,  $\eta_p^w$ , reaching selected depths in the sea during the research period

Rys. 12. Zmiany w okresie badań całodziennych dów energii światła widzialnego w paśmie 400—700 nm —  $\eta_p^w$ , docierających na wybrane głębokości w morzu

lasting for several days in particular months and the whole period, together with standard deviations are listed in Table 2 (columns 5—8). As can be seen, at small depths (0 and 10 m), gradual decrease of the mean diurnal energy doses was observed at specific time intervals from December to March. This was mostly due to irradiance conditions at the surface of the basin, in particular to decreasing sun declination during this period. On the other hand, at greater depths (20 and 30 m, cf. Table 2, columns 7 and 8) this astronomical factors was dominated by optical properties of the water body. Hence, at a depth of 20 m, the highest mean energy was observed in January rather than in December, and at 30 m the highest mean dose was noted in February.

As mentioned in the introduction, solar radiation penetrating the sea is the basic source of energy for primary production of the biomass in the upper layer of a basin, referred to as the euphotic zone. The extent of this zone is usually determined by the compensating depth of photosynthesis in the sea. This depth was shown [2] to be equal to the  $z_e$  depth (eq. 10) reached by 1% of the radiant energy within the maximum transmission band (in this case it is the 525-nm light). Fig. 13 and 14 show time variations of the mean diurnal  $z_e$  values and the distribution of their relative rates of occurrence during the whole period in Ezcurra Inlet.

Average daily ranges of the euphotic zone in the basin considered fluctuated markedly, as did the previously discussed irradiance attenuation coefficients determining the magnitude of  $z_e$ . On the other hand, the average values from observations lasting for several days were relatively constant (cf. Table 2, column 10). The mean range of

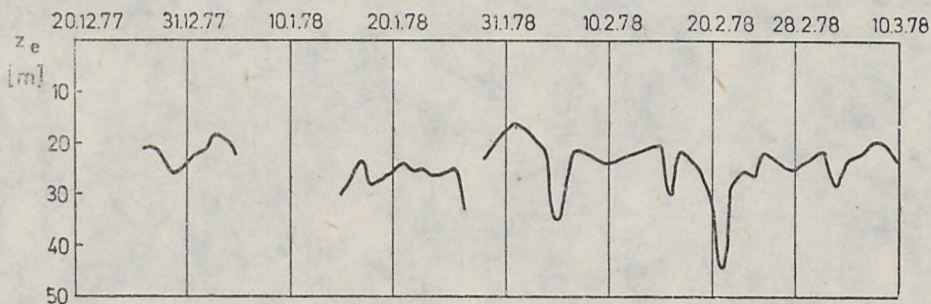


Fig. 13. Variations of mean ranges of the euphotic zone,  $z_e$ , in the sea on particular days during the research period

Rys. 13. Zmiany w okresie badań przeciętnych w poszczególnych dniach zasięgów strefy eufotycznej —  $z_e$ , w morzu

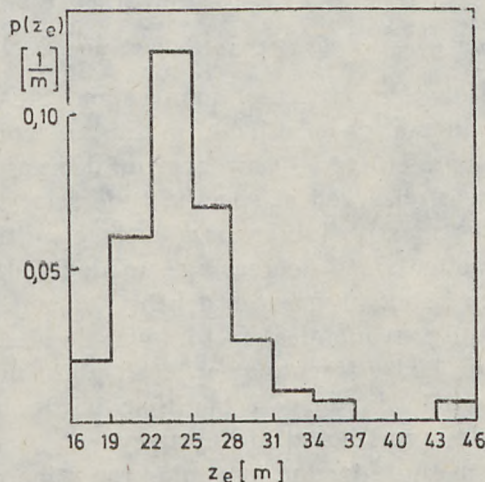


Fig. 14. Distribution of relative frequency of occurrence of ranges of the euphotic zone in the sea

Rys. 14. Rozkład względnych częstotliwości występowania zasięgów strefy eufotycznej w morzu

the euphotic zone in Ezcurra Inlet, determined for the whole research period, was 25 m, which was relatively small as compared with its range in open oceanic waters (about 40 and 140 m in Jerlov's [7] III and I type of waters, respectively) and comparable with that in the open Baltic waters.

Finally, when considering the energetic characteristics of light fields in a basin it is worth mentioning a practical parameter, the function of the transmission of solar radiation,  $P(z)$ . This determines the ratio of radiant energy observed at depth  $z$  to a similar energy reaching the layer

immediately below the surface of a basin. The knowledge of this function (in particular, its variations during a particular season or in a sea region) enables a rough estimate to be made of the doses or irradiance at various depths of the water body on the basis of known, absolute magnitudes of such energy penetrating immediately below the water surface or falling on the surface of the basin (in the latter case, a knowledge is also required of the coefficient of radiation transmission through the sea surface which depends, among other things, on the height of the sun, the relationship between the irradiance with direct solar flux to irradiance with the radiation scattered in the atmosphere, the degree of undulation of the sea surface, etc. Preliminary findings of this case, as well as the results of other papers [1, 5] show, however, that this transmission, with reference to diurnal visible light energy doses at various depths, determined by us, enabled this function to be determined from the expression:

$$P(z) = \frac{\eta_d^w(z)}{\eta_d^w(z=0)}$$

Table 6. Averaged (for observations lasting many days in particular months and the whole research period) functions of transmission of whole-day visible (400—700 nm) irradiance doses into water body of Ezcurra Inlet together with standard deviations of the observed values of these functions

Tab. 6. Średnie (dla wielodniowych obserwacji w poszczególnych miesiącach i dla całego okresu badań) funkcje transmisji w głąb toni wodnej fiordu Ezcurra całodziennych dów promieniowania słonecznego w zakresie widzialnym (400—700 nm) wraz z odchyleniami standardowymi notowanych wartości tych funkcji

Observation days Czas obserwacji	$\langle P(z) \rangle$			
	0—5 m	0—10 m	0—20 m	0—30 m
XII	0.247	0.0685	0.00646	0.000706
	δ 0.017	0.0123	0.00271	0.000444
I	0.248	0.0787	0.0104	0.00172
	δ 0.041	0.0278	0.0076	0.00188
II	0.244	0.0790	0.0114	0.00242
	δ 0.048	0.0341	0.0130	0.00531
III	0.240	0.0735	0.00902	0.00137
	δ 0.034	0.0185	0.00469	0.00117
Total Łącznie	0.245	0.0770	0.0102	0.00183
	δ 0.041	0.0286	0.0098	0.00369

The  $P(z)$  function determined in this manner presents the transmission of the diurnal dose of the 400—700-nm solar radiation in a layer limited by the 0 and  $z$  depths. It can also be taken to be the daily average of downward irradiance within this layer. The calculated mean values of these functions (for observations over periods of several days in particular months and the whole period) at exemplary depths, together with their standard deviations, are shown in Table 6. Comparison of the results for Ezcurra Inlet with those for the Southern Baltic published in [1], shows the transmission functions to be similar in the two basins.

### 5. FINAL REMARKS

The results presented in this paper refer to a specific period and region of exploration. They should therefore be considered as exemplary for the summer period and probably typical for small in-shore fiords (with limited exchange of water masses with the ocean) situated between latitudes 60—65° in the zone of direct influence of glaciers.

The analyses were presented from the aspect of the physical nature of the light inflow to a marine ecosystem. It is, however, worth noting the possibility of practical utilization of the results, as complementary and auxillary for other branches of oceanography, investigated simultaneously during the Second Polish Antarctic Expedition, in view of the dominating role played by sunlight in several processes occurring in the sea. An example of such utilization of the results of optical investigations in biological research is provided by the analysis of primary production of the ecosystem, as well as optical and energetic implications of photosynthesis presented by the present authors in another paper in this volume.

Bogdan WOŹNIAK, Ryszard HAPTER, Barbara MAJ

Polska Akademia Nauk  
Zakład Oceanologii w Sopocie

## DOPŁYW ENERGII SŁONECZNEJ I OŚWIETLENIE STREFY EUFOTYCZNEJ W REJONIE FIORDU EZCURRA W OKRESIE ANTARKTYCZNEGO LATA 1977/1978

### Streszczenie

Przedmiotem badań było naturalne oświetlenie strefy eufotycznej morza w rejonie fiordu Ezcurra latem 1977/1978 r. Badania eksperymentalne przeprowadzono ze statku „Antoni Garnuszewski” podczas II Polskiej Wyprawy Antarktycznej. Na podstawie tych badań dokonano analizy — rozłącznie — warunków oświetlenia na powierzchni morza, współczynników osłabiania oświetlenia w toni wodnej i charakterystyk energetycznych pól światła wewnętrz strefy eufotycznej.

W wyniku tych pomiarów i obliczeń określono zarówno czasowe zmienności wielkości charakteryzujących pola oświetleń w skali dziennej, jak i związane z nimi odpowiednie całodzienne dozy energii światła dla poszczególnych dni w okresie badań. Ze względu na dużą objętość uzyskanego materiału niemożliwa jest w tym artykule kompletna jego prezentacja. Dlatego też ograniczono się tu do przedstawienia jedynie najistotniejszych parametrów, tj. całodziennych dów energii światła słonecznego docierającego do powierzchni morza i na wybrane głębokości w strefie eufotycznej oraz średnich dla poszczególnych dni parametrów optycznych morza i atmosfery. Wyniki te — przedstawione w tab. 1 i na rys. 3, 7, 12, 13 — charakteryzują zmienności pól oświetleń i środowiskowych właściwości optycznych w skali całego okresu badań. Co zaś się tyczy wspomnianych zmian analizowanych wielkości w skali jednego dnia, ograniczono się do prezentacji przykładowych, typowych dla okresu i rejonu badań sytuacji (zob. rys. 1, 9, 10) oraz do przedstawienia wyników odpowiednich statystyk określających dzienne przebiegi parametrów, uśrednione dla wielodniowych obserwacji i całego okresu badań (tab. 2–6 i rys. 2, 6, 11).

Jako charakterystyczne dla analizowanego wypadku stwierdzono silne zróżnicowanie w czasie i fluktuacje naturalnych pól oświetleń w badanym akwenie. Spowodowane one były silnymi zmiennościami czasowymi — zarówno chwilowymi, jak i zachodzącymi z dnia na dzień — warunków optycznych w atmosferze oraz morzu i dotyczyły zarówno składu spektralnego promieniowania dyfundującego w głąb morza (zob. rys. 9), jak i bezwzględnych wielkości energii (rys. 11 i 12).

Spektralny charakter osłabiania oświetlenia w toni wodnej badanego akwenu ilustruje przedstawione na rys. 6 średnie (dla całego okresu badań) widmo współczynnika osłabiania wraz z przedziałem odchyleń standardowych notowanych wartości współczynników. Jak widać, minimum osłabiania w toni wodnej fiordu Ezcurra przypada na światło widmowe o długości fali ok. 525 nm, co jest cechą charakterystyczną dla wód przybrzeżnych klas od 1 do 5 wg optycznej klasyfikacji Jerlova [7]. Również wartości bezwzględne współczynników mieszczą się najczęściej w przedziale charakterystycznym dla tych klas. Jednakże kształty widma  $K_d(\lambda)$  w badanym akwenie zasadniczo odbiegają od podobnych spotykanych w innych morzach. Odstępstwo to polega na znacznie mniejszym, we fiordzie Ezcurra względem innych

akwenów, nachyleniu krzywej w krótkofalowej części widma widzialnego. Sytuacja ta w analizowanym przypadku może być wyjaśniona stosunkowo małą ilością rozpuszczonych w wodzie morskiej substancji organicznych, które silnie absorbowują światło w tej części widma. Tak więc przeważający udział w osłabianiu światła przez składniki mają tu występujące w dużych ilościach zawiesiny (zob. w niniejszym tomie opracowanie Jonasza), które osłabiają światło znacznie bardziej nieselektywnie względem długości fali, głównie przez proces rozpraszania. Potwierdzają to również wyniki uzyskane przez Olszewskiego [12].

Przenikające do morza promieniowanie słoneczne jest zasadniczym źródłem energii podtrzymującym proces produkcji pierwotnej biomasy zachodzący w górnej warstwie akwenu zwanej strefą eufotyczną. Za zasięg tej strefy przyjmuje się najczęściej głębokość kompensującą procesu fotosyntezy w morzu. Jak wykazały badania [2], pokrywa się ona dobrze ze zdefiniowaną równaniem 10 głębokością  $z_e$ , do której dociera 1% energii promieniowania w paśmie o maksymalnej transmisji (w analizowanym wypadku jest to światło o długości fali ok. 525 nm). Na rys. 13 podane są zmiany w okresie badań, przeciętnych dziennych wartości zasięgu  $z_e$ , notowanych we fiordzie Ezcurra. Podobnie jest w wypadku analizowanych wcześniej i determinujących wielkość  $z_e$  współczynników osłabiania oświetleń, przeciętne w poszczególnych dniach zasięgi strefy eufotycznej w badanym akwenie dosyć znacznie fluktuowały, chociaż ich średnie z obserwacji wielodniowych (zob. w kol. 10 tab. 2) okazały się stosunkowo stabilne. Wyznaczony średni dla całego okresu badań zasięg strefy eufotycznej we fiordzie Ezcurra wynosi 23 m, jest stosunkowo mały w porównaniu z zasięgami tej strefy spotykanymi na otwartych wodach oceanicznych, od ok. 40 m w typie III wód oceanicznych do ok. 140 m w typie I [7] i porównywalny ze spotykanym w wodach otwartego Bałtyku.

Przedstawione w tym artykule wyniki dotyczą wybranego okresu i specyficznego rejonu badań. Przeanalizowaną sytuację należy więc traktować jedynie jako przykładową dla okresu letniego i prawdopodobnie typową dla niewielkich przybrzeżnych akwenów fiordowych (z ograniczoną wymianą mas wodnych z oceanem) położonych w szerokościach geograficznych 60–65°, w strefie bezpośredniego wpływu lodowca.

## REFERENCES

1. Czyszek, W., W. Wensierski, J. Dera, *Dopływ i absorpcja energii słonecznej w wodach Bałtyku*, Studia i Materiały Oceanologiczne KBM PAN, 1979, 26.
2. Dera, J., *Charakterystyka oświetlenia strefy eufotycznej w morzu*, Oceanologia, 1971, 1.
3. Dera, J., W. Wensierski, J. Olszewski, *A Two-Detector Integration System for Optical Measurements in the Sea*, Acta Geophys. Pol., 1972, 2.
4. Glagolev, Yu. A., *Spravochnik po fizicheskim parametram atmosfery*, Leningrad 1970.
5. Hapter, R., W. Wensierski, *Naturalne oświetlenie strefy eufotycznej Bałtyku*, Studia i Materiały Oceanologiczne KBM PAN, 1973, 7.
6. Egorov, B. N., T. V. Kirillova, *Summarnaya radiatsiya nad okeanom v usloviyah bezoblachnogo neba*, Trudy G.G.O., 1973, 297.

7. Jerlov, N. G., *Optical oceanography*, Elsevier Publ. Company, Amsterdam 1968.
8. Jonasz, M., *Particulate matter in the Ezcurra Inlet: Concentration and size distributions*, Oceanologia, 1983, 15.
9. Mandelli, E. F., P. R. Burkholder, *Primary Productivity in the Gerlache and Bransfield Straits of Antarctica*, J. Marine Res., 1966, Vol. 24, No. 1.
10. Montwiłł, K., *Spektrointegrator wielokanałowy do badań optycznych w morzu*, Studia i Materiały Oceanologiczne KBM PAN, 1975, 10.
11. Olszewski, J., *Przystawka spektrofotometryczna do analizy widmowej naturalnego oświetlenia w morzu*, Oceanologia, 1975, 10.
12. Olszewski, J., *The basic optical properties of the water in the Ezcurra Inlet*, Oceanologia, 1983, 15.
13. Słomka, J., K. Słomka, *Influence of clouds on the biological efficiency of solar radiation*, Materiały i Prace Instytutu Geofizyki PAN, 1972, 49.
14. *Solar Radiation and Radiation Balance Data (the World Network)*, Hydrometeorological Publishing House, Leningrad 1970.
15. Tooming H. G., B. Y. Gulaev, *Metodika izmereniya fotosinteticheski aktivnoi i radiatsii*, Moskva 1967.
16. Węsierski, W., B. Woźniak, *Optical Properties of Water in Antarctic Waters*, Pol. Arch. Hydrobiol., 1978, Vol. 25, No 3.
17. Woźniak B., K. Montwiłł, *Metody i techniki pomiarów optycznych w morzu*, Studia i Materiały Oceanologiczne KBM PAN, 1973, 7.

Manuscript received in 1979